Chaotic Modeling and Simulation (CMSIM) **1: 52-59, 2016**

Stochastic Calculations for Fibre Raman Amplifiers with Randomly Varying Birefringence

Vladimir L. Kalashnikov[1], Sergey Sergeyev[1]

[1] Aston University, Institute of Photonic Technologies, School of Engineering & Applied Science, Aston Triangle, Birmingham, B4 7ET, UK
(E-mail: v.kalashnikov@aston.ac.uk)

Abstract. For the first time for the model of real-world forward-pumped fibre Raman amplifier with the randomly varying birefringence, the stochastic calculations have been done numerically based on the Klöden-Platen-Schurz algorithm. The results obtained for the averaged gain and gain fluctuations as functions of polarization mode dispersion (PMD) parameter agree quantitatively with the results of previously developed analytical model. Simultaneously, the direct numerical simulations demonstrate an increased stochastization (maximum in averaged gain variation) within the region of the polarization mode dispersion parameter of 0.01÷0.1 ps/km$^{1/2}$. The results give an insight into margins of applicability of a generic multi-scale technique widely used to derive coupled Manakov equations and allow generalizing analytic model with accounting for pump depletion, group-delay dispersion and Kerr-nonlinearity that is of great interest for development of the high-transmission-rates optical networks.

Keywords: Stochastic modeling, Raman amplifiers, Fibre optic communications.

1 Introduction

Rapid progress in overall capacity of optical networks based on the distributed fibre Raman amplifiers [1] (FRAs) faces the challenge of increased transmission impairments related to polarization depend gain (PDG) and gain fluctuations (GF), e.g. dependence of the Raman gain on the input states of polarization (SOP) and random nature of birefringence in optical fibres [2-5]. As was found previously [2, 3], the randomly varying birefringence contributes essentially into GF by de-correlating the signal and pump SOPs that prevents polarization pulling of the signal SOP to the pump one. As a result, GF takes a maximum value as a function of PMD parameter [2, 3] that is related to phenomena of

Revised received: 14 January 2016 / Accepted: 26 January 2016

ISSN 2241-0503

stochastic resonance (SR), dynamic localization phenomena and escape from a metastable state in an excitable system [4, 6-9].

2 Model of the Raman-scattering Induced Polarization Phenomena in Presence of the Stochastic Birefringence

To validate our previously developed analytical models [3, 4] and application of multiple-length-scale technique developed by Menyuk [10] to study PDG and GF in FRAs, for the first time to our knowledge we present the results of direct stochastic calculations of PDG and GF in FRAs. The starting point is the coupled Manakov-PMD equations describing co-propagation of signal and pump waves in a FRA [2,5,11]:

$$\begin{aligned} & i\frac{\partial|A_s\rangle}{\partial z}+\beta_s[\cos(\theta)\,\sigma_3+\sin(\theta)\,\sigma_1]|A_s\rangle+i\frac{\alpha_s}{2}|A_s\rangle+ \\ & i\beta_s'[\cos(\theta)\,\sigma_3+\sin(\theta)\,\sigma_1]\frac{\partial|A_s\rangle}{\partial t}-\frac{\beta_s''}{2}\frac{\partial^2|A_s\rangle}{\partial t^2} \\ & \quad+\frac{\gamma_{ss}}{3}[2\langle A_s|A_s\rangle+|A_s^*\rangle\langle A_s^*|]|A_s\rangle \\ & \quad+\frac{2\gamma_{sp}}{3}\left[2\langle A_p|A_p\rangle+|A_p\rangle\langle A_p|+|A_p^*\rangle\langle A_p^*|\right]|A_s\rangle \\ & \quad-\frac{ig_R}{2}|A_p\rangle\langle A_p|A_s\rangle=0, \end{aligned} \tag{1}$$

$$\begin{aligned} & i\frac{\partial|A_p\rangle}{\partial z}+\beta_p[\cos(\theta)\,\sigma_3+\sin(\theta)\,\sigma_1]|A_p\rangle+i\frac{\alpha_p}{2}|A_p\rangle+ \\ & i\beta_p'[\cos(\theta)\,\sigma_3+\sin(\theta)\,\sigma_1]\frac{\partial|A_p\rangle}{\partial t}-\frac{\beta_p''}{2}\frac{\partial^2|A_p\rangle}{\partial t^2} \\ & \quad+\frac{\gamma_{pp}}{3}[2\langle A_p|A_p\rangle+|A_p^*\rangle\langle A_p^*|]|A_p\rangle \\ & \quad+\frac{2\gamma_{sp}}{3}\left[2\langle A_s|A_s\rangle+|A_s\rangle\langle A_s|+|A_s^*\rangle\langle A_s^*|\right]|A_p\rangle \\ & \quad+\frac{ig_R}{2}\frac{\omega_p}{\omega_s}|A_s\rangle\langle A_s|A_p\rangle=0. \end{aligned}$$

Here

$$\sigma_1=\begin{bmatrix}0 & 1\\ 1 & 0\end{bmatrix},\sigma_2=\begin{bmatrix}0 & -i\\ i & 0\end{bmatrix},\sigma_1=\begin{bmatrix}1 & 0\\ 0 & -1\end{bmatrix},|A_k\rangle=\left(A_{kx},A_{ky}\right)^T$$

are the polarization vectors for pump ($k = p$) and signal ($k = s$), respectively. $\beta_{s,p} = 2\pi/L_{s,p}$ is the corresponding birefringence strength ($L_{s,p}$ are the beat lengths for pump and signal at the frequencies ω_p and ω_s, respectively), $\beta'_{s,p}$ are the group-delays, and $\beta''_{s,p}$ are the group-delay dispersions, $\gamma_{k,m}$ are the self- and cross-phase modulation coefficients ($k = s, p; m = s, p$). $\alpha_{p,s}$ are the attenuation coefficients for pump and signal, respectively. At last, g_R is the Raman gain coefficient and θ is the angle defining the birefringence axis [3].

For comparatively small propagation distances ($z < 20$ km), long pulses (>2.5 ps), small pump and signal powers ($P_{in} < 1$ W and $s_0 < 10$ mW, respectively) one may neglect group-delay, its dispersion and nonlinear effects in a system. Then, the rotation $|A_i\rangle = R|a_i\rangle, R = \begin{bmatrix} \cos(\theta/2) & \sin(\theta/2) \\ -\sin(\theta/2) & \cos(\theta/2) \end{bmatrix}$ results in the equations for the pump and signal Jones vectors $|a_p\rangle$ and $|a_s\rangle$:

$$i\frac{d|a_s\rangle}{dz} + \Sigma_s|a_s\rangle + i\frac{\alpha_s}{2}|a_s\rangle - i\frac{g_R}{2}|a_p\rangle\langle a_p|a_s\rangle = 0, \qquad (2)$$

$$i\frac{d|a_p\rangle}{dz} + \Sigma_p|a_p\rangle + i\frac{\alpha_p}{2}|a_p\rangle = 0,$$

where $\Sigma_k = \begin{bmatrix} \beta_i & -i\theta_z \\ i\theta_z & -\beta_i \end{bmatrix}, \theta_z \equiv \frac{\partial\theta}{\partial z} = g_\theta$, k-index corresponds to pump (p) or signal (s), and g_θ is a Wiener process defining the birefringence stochastic: $\langle g_\theta(z)\rangle = 0, \langle g_\theta(z)g_\theta(z')\rangle = \sigma_\theta^2\delta(z-z')$, and $\sigma_\theta^2 = 1/L_c$, where L_c is the correlation length for the birefringence vector fluctuations. Transition to the reference frame in the Stokes space where the local birefringence vectors $\overrightarrow{\boldsymbol{W}_i}$ have the components $(\beta_i, 0, 0)$ [3] results in the system of stochastic differential equations of Stratanovich type for the unit vectors $\vec{\boldsymbol{s}}$ and $\vec{\boldsymbol{p}}$ defining the signal and pump SOPs and their scalar product $x = \vec{\boldsymbol{s}} \cdot \vec{\boldsymbol{p}}$:

$$\frac{d(s_0\vec{\boldsymbol{s}})}{dz} = \frac{g_R}{2}P_0(z)s_0\vec{\boldsymbol{p}} + \begin{pmatrix} s_2 \\ -s_1 \\ 0 \end{pmatrix}s_0 g_\theta + s_0\beta_s\begin{pmatrix} 0 \\ -s_3 \\ s_2 \end{pmatrix},$$

$$\frac{ds_0}{dz} = \frac{g_R}{2}P_0(z)x(z)s_0(z), \qquad (3)$$

$$\frac{d(s_0 x)}{dz} = \frac{g_R}{2} P_0(z) s_0 - (\beta_p - \beta_s)(p_3 s_2 - p_2 s_3) s_0,$$

$$\frac{d\vec{\boldsymbol{p}}}{dz} = \begin{pmatrix} p_2 \\ -p_1 \\ 0 \end{pmatrix} g_\theta + \beta_p \begin{pmatrix} 0 \\ -p_3 \\ p_2 \end{pmatrix}.$$

Here s_0 is a length of signal Stokes vector normalized to $\exp\left(\int_0^L \frac{g_R P(z)}{2} dz - \alpha_s L\right)$, L is the fibre length, and $P_0(z) = P_{in} \exp(-\alpha_p z)$. The average gain $\langle G \rangle$ and the PDG parameters are defined as $\langle G \rangle = 10 \log(\langle s_0(L) \rangle / s_0(0))$ and $PDG = 10 \log(\langle s_{0,max}(L) \rangle / \langle s_{0,min}(L) \rangle)$, respectively.

Equations (3) can be averaged over both regularly (the scales are defined by $L_{s,p}$) and randomly (the scale is defined by L_c) varying birefringence that results in [3]:

$$\frac{d\langle s_0 \rangle}{dz'} = \frac{g_R P_{in} L}{2} \exp(-\alpha_s z') \langle x \rangle,$$

$$\frac{d\langle x \rangle}{dz'} = \frac{g_R P_{in} L}{2} \exp(-\alpha_s z') \langle s_0 \rangle - \beta_s L \langle y \rangle, \qquad (4)$$

$$\frac{d\langle y \rangle}{dz'} = \beta_s L (\langle x \rangle - p_1(0) s_1(0) \exp(-z' L / L_c)) - \langle y \rangle L / L_c,$$

where $z' = z/L$. Further generalization of this analytical approach [4] allows characterizing a system in more complete way. In particular, the standard deviations for both $\langle G \rangle$ and $\langle x \rangle$ can be obtained.

Eqs. (3) have been solved with the Wolfram Mathematica 9.0 computer algebra system by the built-in Klöden-Platen-Schurz method with the propagation step $\Delta z = 10^{-4} \min(L_c, L_i)$. The averaging procedure was performed over an ensemble of 100 stochastic trajectories. We have used the following parameters: g_R =0.8 $W^{-1}km^{-1}$, s_0 =10 mW, P_{in} =1 W, L =5 km, L_c =100 m. Stokes parameters for the pump and the input signal fields corresponding to the maximum and minimum gain were $\vec{\boldsymbol{p}}$=(1,0,0), $\vec{\boldsymbol{s}}$=(1,0,0) and $\vec{\boldsymbol{p}}$=(1,0,0), $\vec{\boldsymbol{s}}$=(–1,0,0), respectively.

3 Results and Discussion

In this work, for the first time to our knowledge we present the results of direct stochastic calculations of PDG and GF in FRAs.

In terms of SR, correlation length L_c and beat lengths $L_{s,p}$ play roles of inverse noise strength and frequency of external periodic modulation, respectively [4, 6]. The PMD parameter is defined as $\sqrt{2L_c}\lambda_s/\pi c L_s$ (c is the light speed, λ_s is the signal wavelength) and so according to the SR theory there is some PMD value at which GFs, i.e. the relative gain standard deviation $\sigma/\langle G\rangle$ is minimal. However, the gain fluctuations are resonantly enhanced in the vicinity of $L_b \approx L_c/4$ (red curve in Fig. 1 (a)). Such a growth of GFs corresponds to enhancement of "wondering" of stochastic trajectories for s_0 and $\langle x\rangle$, as it is demonstrated by insets in Fig. 1 (b). Thus, the phenomenon reported can be termed *stochastic anti-resonance* (SAR).

Since the PMD growth activates escape from polarization pulling SOP corresponding to $\langle x\rangle \to 1$ (black solid curve in Fig. 2), the maximum averaged gain $\langle G\rangle$ decreases in the quantitative agreement with the analytical model of Eqs. (4) (black solid and dashed curves in Fig. 1 (a)). Simultaneously, a de-correlation of the pump-signal SOP (dashed red curve for the standard deviation $\sigma_{\langle x\rangle}$ in Fig. 2) allows reducing the PDG with the PMD growth (black curve in Fig. 1 (b)).

An enhancement of stochasticity is illustrated by anti-resonance valley in the dependence of the Hurst parameter H [14] on the PMD (inset in Fig. 2), when an initially highly correlated SOP with $H \approx 1$ tends to become Brownian ($H \to 0.5$). Such a switch between the statistical scenarios is typical for SAR, when the variance increases with growth of variability in a system [15].

Further growth of PMD suppresses the GFs (red curve in Fig. 1 (a)) and increases the Hurst parameter for $\langle x\rangle$ (inset in Fig. 2) although the pump and signal SOPs remain de-correlated (red dashed curve for $\sigma_{\langle x\rangle}$ in Fig. 2). Such a scenarios corresponds to the escape from a pulling state when the gain and signal SOPs evolve independently and substantially faster than the random changes of birefringence (i.e. $L_i \ll L_c$). Such an intensification of polarization evolution affects the

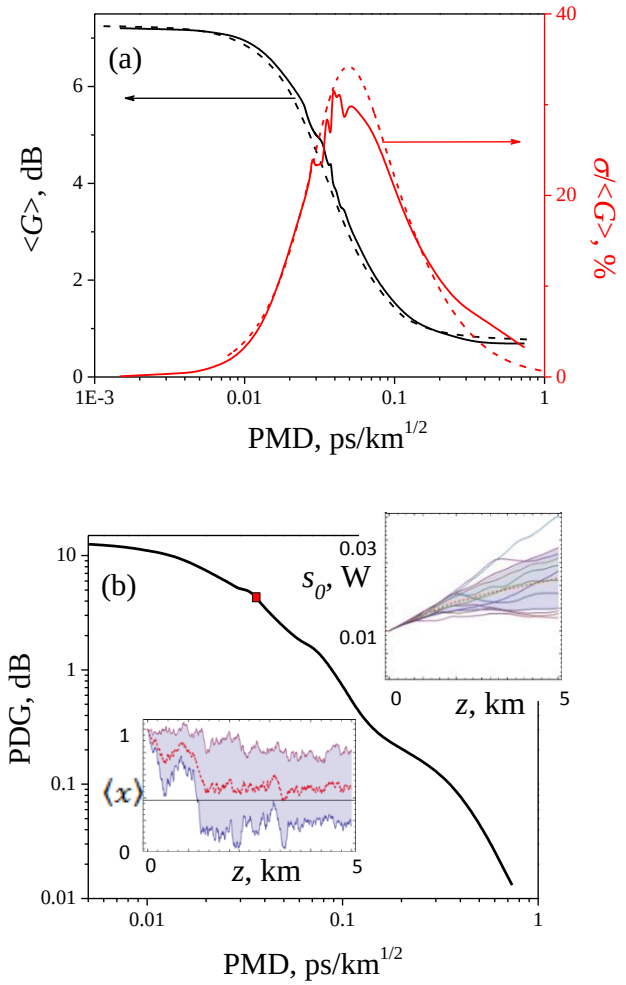

Fig. 1. (a): the averaged maximum gain $\langle G \rangle$ vs. PMD from numerical simulations (solid black curve) and analytical model of Eqs. (4) (dashed black curve) as well as numerical (solid red curve) and analytical [4] (dashed red curve) relative standard deviation $\sigma/\langle G \rangle$. (b): the PDG parameter vs. PMD. The inserts correspond to red square, where the standard deviation is maximum, and show the stochastic trajectories of signal s_0 as well as the correlation of signal and pump SOPs $\langle x \rangle$ (dashed curves are the ensemble averages, filled regions are bounded by the corresponding standard deviation σ).

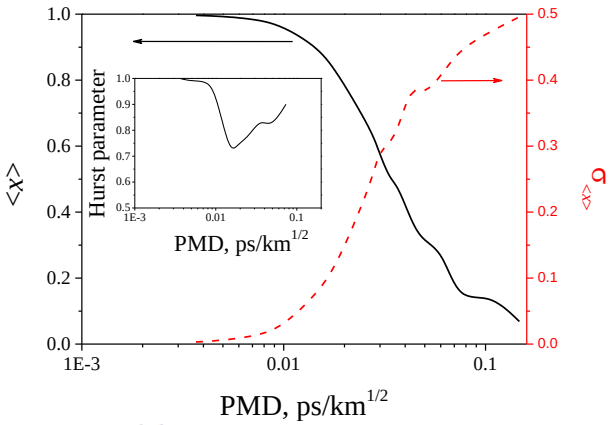

Fig. 2. Dependencies of $\langle x \rangle$ (black solid curve), its standard deviation $\sigma_{\langle x \rangle}$ (red dashed curve), and the corresponding Hurst parameter (inset) on the PMD parameter for $\vec{p}$=(1,0,0) and $\vec{s}$=(1,0,0).

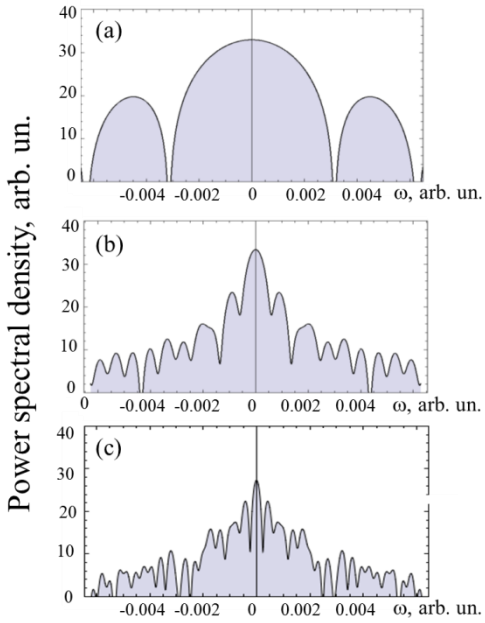

Fig. 3. Power density spectra of $\langle x \rangle$ for $\vec{p}$=(1,0,0) and $\vec{s}$=(1,0,0) and the signal beat lengths L_s of 200 (a), 20 (b) and 10 m (c), respectively.

power spectral density of $\langle x \rangle$ which demonstrates a dramatic increase in a number of additional frequencies with the PMD growth (Fig. 3).

4 Conclusion

In conclusion, the Stratanovich-type equations describing Raman amplification in fibres in the presence of stochastic birefringence have been solved directly for the first time to our knowledge. The results obtained revealed a transition between different stochastic scenarios of mean gain and its fluctuations. It is shown that the PMD growth induces an escape from the regular metastable state of the pump and signal SOPs pulling to the state of de-correlated but comparatively regular SOPs. Such an escape can be characterized as the "*stochastic anti-resonance*" accompanied by substantial enhancement of GFs and quasi-Brownian evolution of the pump-signal coupling. A range of PMD parameters corresponding to such stochastization is typical for modern FRAs and, thereby, is of interest for high-capacity un-repeatered firbe networks. The demonstrated quantitative agreement of the numerical results with the analytical ones based on multi-scale averaging techniques promises developing a generalized approach to design and optimization of FRAs.

Acknowledgments

Support of the FP7-PEOPLE-2012-IAPP (project GRIFFON, No. 324391) is acknowledged. The computational results have been achieved using the Vienna Scientific Cluster (VSC).

References

1. J. Cheng et al., "Relative Phase noise-Induced Phase Error and System Impairment in Pump Depletion/Nondepletion Regime," J. Lightw. Technol. **32**, 2277-2286 (2014).
2. Q. Lin, G.P. Agrawal, "Vector theory of stimulated Raman scattering and its application to fiber-based Raman amplifiers," J. Opt. Soc. Am. B **20**, 1616 (2003).
3. S. Sergeyev, S. Popov, A.T. Friberg, "Modelling polarization-dependent gain in fiber Raman amplifiers with randomly varying birefringence," Optics Commun. **262**, 114 (2006).

4. S.V. Sergeyev, "Activated polarization pulling and de-correlation of signal and pump states of polarization in a fiber Raman amplifier," Optics Express **19**, 24268 (2011).
5. V. V. Kozlov, J. Nuño, J. D. Ania-Castañón, and S. Wabnitz, "Theory of fiber optic Raman polarizers," Opt. Lett. **35**, 3970-3972 (2010).
6. L. Gammaitoni, P. Hänggi, P. Jung, F. Marchesoni, "Stochastic resonance," Rev. Mod. Phys. **70**, 223 (1998).
7. P. Hanggi, "Escape from a metastable state," J. Statistical Physics **42**, 105-148 (1986).
8. B. Lindner, J. Garsia-Ojalvo, A. Neiman, L. Schimansky-Greif. "Effects of noise in excitable systems," Phys. Reports **392**, 321-424 (2004).
9. M.I. Dykman, B. Golding, L.I. McCann, V.N. Smelyanskiy, D.G. Luchinsky, R. Mannella, P.V.E. McClintock. "Activated escape of periodically driven systems," Chaos **11**, 587–594 (2001).
10. P.K.A. Wai, C.R. Menyuk, "Polarization mode dispersion, decorrelation and diffusion in optical fibers with randomly varying birefringence," J. Lightwave Technol. **14**, 148 (1996).
11. V.V. Kozlov, J. Nuño, J.D. Ania-Castañón, and S. Wabnitz, "Multichannel Raman polarizer with suppressed relative intensity noise for wavelength division multiplexing transmission lines," Opt. Lett. **37**, 2073-2075 (2012).
12. C.R. Menyuk, "Application of multiple-length-scale methods to the study of optical fiber transmission," J. Engineering. Math. **36**, 113-136 (1999).
13. C.R. Menyuk, B.S. Marks, "Interaction of Polarization Mode Dispersion and Nonlinearity in Optical Fiber Transmission Systems," J. Light. Techn. **24**, 2806- 2826 (2006).
14. *Mathematics of Complexity and Dynamical Systems*. R.A. Meyers (Ed.), (Springer, 2009).
15. *Computational Methods in Stochastic Dynamics*. M. Papadrakakis, G. Stefanou,V. Papadopoulos (Eds.), Vol. 2 (Springer, 2013).